

Smoothing of an Irregular Anode Surface

If a particular cathode shape is chosen for an ECM operation, the anode form should eventually become approximately complementary to it. Studies of the shaping process of ECM are often concerned with the variation in the shape of the anode as machining proceeds, and with the machining time required to achieve the steady-state shape on the anode. They should also deal with the influence of overpotentials, and with the effects of the electrolyte flow. (The question of flow has yet to be tackled in any definitive fashion, and is not considered in this chapter.)

The simplest case of shaping which allows these problems to be studied is anodic smoothing. Here the cathode has a flat plane face, and the anode surface initially carries surface irregularities. These are gradually removed by ECM, so that eventually the anode surface also becomes flat, and then, of course, resembles the cathode shape. The practical analogy of this problem is electrochemical deburring, in which surface irregularities are removed electrochemically from an anode workpiece.

6.1 Basic equations

Three basic equations are used:

(i) Laplace's equation

$$\nabla^2 \phi = 0 \quad (6.1)$$

the solution of which will give the potential ϕ at any point in the electrolyte, particularly at the electrode surfaces.

(ii) Ohm's law

$$J = -\kappa_e \nabla \phi \quad (6.2)$$

where J , the current density, will be found from the potential known from (6.1), κ_e being the electrolyte conductivity.

(iii) Faraday's law

$$\dot{r}_a = \frac{AJ}{zF\rho_a} \quad (6.3)$$

which will be used to give the anode recession rate \dot{r} , A being the atomic weight, z the valency, ρ_a the density of the anode metal, and F is Faraday's constant.

The conditions under which these equations can be used – the 'quasi-steady model' of the ECM process – have been investigated in some detail [1, 2]. The boundary conditions for the potential at the electrodes, and the conditions under which Ohm's law and Faraday's law are applicable, are now discussed.

6.2 Potential boundary conditions

If the electrode surfaces are equipotentials, then the boundary conditions are

$$\phi = 0 \text{ at the cathode} \quad (6.4)$$

$$\phi = V \text{ at the anode} \quad (6.5)$$

where V is the applied potential difference. However, we have seen in Chapter 3 that the reactions at both electrodes cause current density-dependent overpotentials. Their presence at the electrodes alters the boundary conditions to

$$\phi = f(J) \text{ at the cathode}$$

$$\phi = V - g(J) \text{ at the anode}$$

where $f(J)$ and $g(J)$ are arbitrary functions for the cathodic and anodic overpotentials respectively.

6.3 Applicability of Ohm's law and Faraday's law

In Chapter 3, we saw that the potential drop across the diffusion layer, associated with the concentration overpotential, is ohmic. In the bulk electrolyte, outside the diffusion layer, all concentration gradients

can be assumed to be destroyed by the agitation of the electrolyte. Accordingly, Ohm's law can be applied in the form $J = \kappa_e E$ where κ_e is the bulk conductivity and E is the electric field. If the diffusion layer thickness and potential drop across it are assumed to be sufficiently small, the conductivity can be assumed to have its bulk value everywhere. The conductivity is also assumed to remain constant everywhere. Joule heating and the formation of hydrogen gas bubbles which, as we have seen, respectively increase and decrease the effective conductivity are assumed to be suppressed by sufficient agitation of the electrolyte.

The use of Faraday's law implies that all the current at the anode is used to dissolve the metal; that is, no other reaction (e.g. oxygen evolution) occurs there.

With these conditions and assumptions, certain solutions of the electrochemical shaping problem are possible. These involve the solution of an elliptic differential equation with moving boundaries. In general, this is difficult; however, if the boundaries are assumed to change so slowly that their motion may be ignored at any given time, then the equation may be solved for any instant of time. From this solution, further equations can be derived which describe the behaviour of the boundary over the next small period of time, when Laplace's equation may again be solved, and so on.

The most tractable cases give rise to boundary-describing equations which are 'self-similar' [3]. These do not involve time explicitly, and may be transformed into equations which do not depend explicitly on the shape of the anode surface. Such cases are considered for

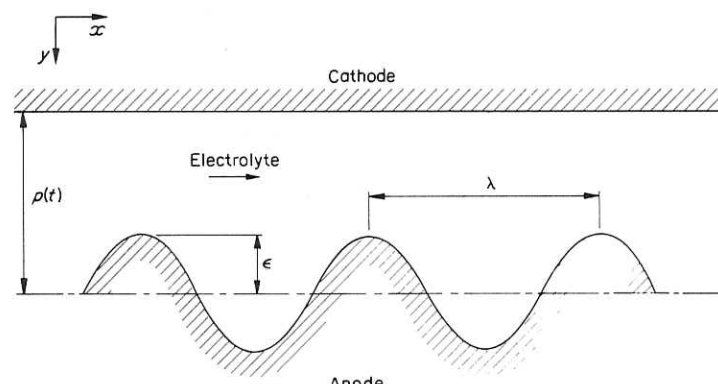


Fig. 6.1 Configuration of electrodes

two-dimensional forms, although the extension to three dimensions will also be outlined. The work will be developed initially without the complication of overpotential effects, i.e. at the cathode a boundary condition $\phi = 0$, and at the anode $\phi = V$, will be assumed. After the physical and mathematical principles have been fully considered, the effect of overpotentials will be included.

6.4 The basic problem

We investigate the smoothing of small irregularities on the anode surface, the configuration of the electrodes being shown in Fig. 6.1. Sinusoidal irregularities of wavelength $\lambda (= 1/k)$, k being the wave number) are considered.

Suppose the plane cathode is given by

$$y = 0 \quad (6.6)$$

and the anode by

$$y = p + \epsilon \sin kx \quad (6.7)$$

where the quantity p is the 'average gap' between the electrodes. The gross behaviour of the anode surface will later be determined by this parameter. The maximum amplitude of the irregularities is given by ϵ , the initial value being $\epsilon(0)$. Initial values of p and ϵ are assumed known; we investigate their subsequent behaviour. It is assumed that

$$\epsilon \ll p \quad (6.8)$$

Initially a solution is sought for Laplace's equation in two dimensions:

$$\frac{\partial^2 \phi}{\partial x^2} + \frac{\partial^2 \phi}{\partial y^2} = 0 \quad (6.9)$$

with the boundary conditions

$$\phi = 0 \quad \text{on } y = 0 \quad (6.10)$$

$$\phi = V \quad \text{on } y = p + \epsilon \sin kx \quad (6.11)$$

Expansion of the solution in terms of the small parameter $\epsilon(0)/p$ gives (to first order in $\epsilon(0)/p$):

$$\phi = \phi_0 + \frac{\epsilon(0)}{p} \phi_1 \quad (6.12)$$

where ϕ_0 is the potential between two plane electrodes at a distance p apart, and ϕ_1 is a non-singular perturbation. The potential ϕ_0 satisfies Laplace's equation, with the boundary conditions

$$\phi_0 = 0 \quad \text{on } y = 0 \quad (6.13)$$

$$\phi_0 = V \quad \text{on } y = p \quad (6.14)$$

The solution is

$$\phi_0 = \frac{Vy}{p} \quad (6.15)$$

ϕ_1 is now chosen to satisfy Laplace's equation, with the boundary conditions

$$\phi_1 = 0 \quad \text{on } y = 0 \quad (6.16)$$

$$\phi_0 + \frac{\epsilon(0)}{p} \phi_1 = V \quad \text{on } y = p + \epsilon \sin kx \quad (6.17)$$

Now, on $y = p + \epsilon \sin kx$,

$$\phi_0 = V + \frac{V\epsilon}{p} \sin kx \quad (6.18)$$

the second boundary condition becomes

$$\phi_1 = -\frac{V\epsilon}{\epsilon(0)} \sin kx \quad (6.19)$$

Separation of variables and application of the first boundary condition give

$$\phi_1 = A \sin kx \sinh ky \quad (6.20)$$

where the constant A is to be determined. Applying the second boundary condition (6.19), we obtain, to first-order approximation in $\epsilon(0)/p$:

$$A = -\frac{V}{\sinh kp} \left(\frac{\epsilon}{\epsilon(0)} \right) \quad (6.21)$$

From Equations (6.12), (6.15), and (6.21), the expression for the potential is obtained:

$$\phi = \frac{Vy}{p} - \frac{V\epsilon}{p} \frac{\sin kx \sinh ky}{\sinh kp} \quad (6.22)$$

6.5 Behaviour of anode surface and of surface irregularities

By the use of this expression for ϕ , a set of equations can be derived which describes separately the behaviour of the anode surface and the behaviour of the irregularities. On the anode surface, consider dy_a/dt , the reduction rate in the vertical direction. (Here, and subsequently, the subscript denotes evaluation at the anode surface.) The field in this direction is $-\partial\phi/\partial y$. If the anode surface is described by a vector function $r_a(x, y)$, then, from Ohm's law and Faraday's law, we obtain

$$\frac{dr_a}{dt} = M \nabla \phi_a \quad (6.23)$$

where $M (= A\kappa_e/Fz\rho_a$, ρ_a being the anode metal density) is a constant. The vertical component of Equation (6.23) is

$$\frac{dy_a}{dt} = M \frac{\partial \phi_a}{\partial y} \quad (6.24)$$

The field at the top and foot of the irregularities is now examined. At the top, $x = (\pi/k)(2n + 3/2)$ with $n = 0, 1, 2, \dots$; $y = p - \epsilon$. Here, the field has no x component, and is given by

$$\begin{aligned} \frac{\partial \phi}{\partial y} &= \frac{V}{p} \frac{V\epsilon k}{p} \frac{\sin(3\pi/2) \cosh k(p - \epsilon)}{\sinh kp} \\ &\simeq \frac{V}{p} \left[1 + \epsilon k \left(\frac{\cosh kp \cosh k\epsilon}{\sinh kp} + \frac{\sinh kp \sinh k\epsilon}{\sinh kp} \right) \right] \\ &\simeq \frac{V}{p} (1 + \epsilon k \coth kp) \end{aligned}$$

Neglected, as before, are terms of order higher than the first in ϵ/p .

Next, Equation (6.24) is used to calculate the amount of metal removed from the top and foot of the irregularity. In time dt the top of the irregularity will have been lowered by an amount $d(p - \epsilon)$, where

$$d(p - \epsilon) = \frac{MV}{p} (1 + \epsilon k \coth kp) dt \quad (6.25)$$

Similarly, the reduction in height of the foot of the irregularity in time dt is given by

$$d(p + \epsilon) = \frac{MV}{p}(1 - \epsilon k \coth kp)dt \quad (6.26)$$

The average of these two quantities is the reduction in height of the average anode surface, causing an increase in the average gap due to ECM. This reduction is offset by a decrease in the average gap due to the forward movement of the cathode, assumed constant at rate f . Using Equations (6.25) and (6.26), we obtain

$$\frac{dp}{dt} = \frac{MV}{p} - f \quad (6.27)$$

in agreement with elementary ohmic theory for two plane electrodes at the average gap [see Equation (5.3)].

The difference between the quantities obtained in Equations (6.25) and (6.26) divided by 2, is the decrease in height of the irregularity in time dt ; we obtain

$$\frac{d\epsilon}{dt} = -\frac{MVk}{p} \coth kp \epsilon \quad (6.28)$$

as the differential equation describing the time behaviour of the height of the irregularities.

We have thus derived, from our solution of Laplace's equation, a set of equations describing separately the gross behaviour of the anode surface and the behaviour of the irregularities. Solving Equation (6.27), we obtain, as usual;

$$t = \frac{1}{f} \left[p(0) - p + \frac{MV}{f} \ln \frac{MV - fp(0)}{MV - fp} \right] \quad (6.29)$$

which may be expressed as

$$t = \frac{1}{f} \left[p(0) - p + p_e \ln \frac{p_e - p(0)}{p_e - p} \right] \quad (6.29a)$$

where $p(0)$ is the initial gap, and $p_e = MV/f$ is the equilibrium gap for the condition specified. Equation (6.29) gives p as an implicit function of t .

Equation (6.27) is quite basic, and has been derived in Chapter 5. Briefly, we recollect that, if $p(0)$ is greater than p_e , then p is always

greater than p_e , and tends to it asymptotically, and vice versa if $p(0)$ is less than p_e .

From Equation (6.28), on transformation:

$$\frac{d\epsilon}{dp} = \frac{d\epsilon}{dt} \frac{dt}{dp} = -\frac{MVk}{MV - fp} \coth kp \epsilon$$

which yields

$$\epsilon = \epsilon(0) \exp \left[-MVk \int_{p(0)}^p \frac{\coth ks}{MV - fs} ds \right] \quad (6.30)$$

provided that dp/dt is not zero, i.e. the process is not being carried out at the equilibrium gap. The formula (6.30) gives ϵ as a function of p , and hence implicitly as a function of time. Note that, as expected ϵ decreases, whether p is increasing or decreasing to its equilibrium value.

Two cases of interest are tractable, depending on the value of the parameter kp .

6.5.1 Short-wavelength irregularities

For the short-wavelength case ($kp \gg 1$), the wavelength is small compared with the gap width. Since $\coth kp$ can be taken to be unity, Equation (6.30) becomes

$$\epsilon(p) = \epsilon(0) \left(\frac{MV - fp(0)}{MV - fp} \right)^{-MVk/f} \quad (6.31)$$

provided that p does not assume its equilibrium value MV/f . Here the dependence of ϵ on p is a power of the quantity $[MV - fp(0)]/[MV - fp]$, and the index depends linearly on the wave number, i.e. the shorter the wavelength, the more quickly are the irregularities dissolved. The significance is discussed more fully in the next section.

6.5.2 Long-wavelength irregularities

In the long-wavelength case ($kp \ll 1$), Equation (6.30) gives

$$\epsilon = \epsilon(0) \frac{p(0)(MV - fp)}{p[MV - fp(0)]} \quad (6.32)$$

(again with the condition $p \neq MV/f$). This is identical with the simple formula for the reduction of a single step on the anode (i.e. assuming

that the current travels only normally between the electrodes). The result is expected, since, with long-wavelength irregularities, the crests and troughs may be considered to be sections of plane electrodes at different distances from the cathode (Fig. 6.2). The similarity is also discussed more fully below.

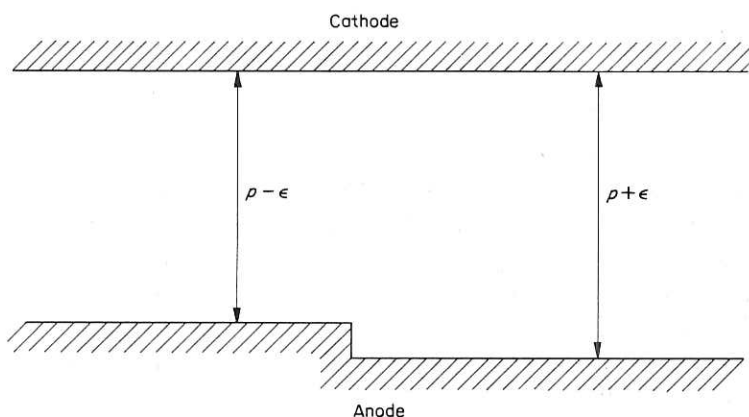


Fig. 6.2 Simple stepped anode (approximation of long-wavelength irregularities; Section 6.5.2)

For equilibrium gap conditions, the solutions of Equations (6.27) and (6.28) are

$$p = \frac{MV}{f} \quad (6.33)$$

and

$$\epsilon = \epsilon(0) \exp\left[-\left(\frac{MVk}{p} \coth kp\right)t\right] \quad (6.34)$$

In later examples, such gap conditions are used.

6.6 Field concentration effects

In a simple theory the field lines across the gap may be considered to be parallel, and the rate of reduction of the irregularities may be obtained by an ohmic theory based on the differences in gap size between corresponding points on the electrodes. The present theory accounts for the field concentration effects: the field at a point where the curvature of the electrode surface is large and convex is

much greater than the field at a plane surface. Since short-wavelength irregularities have a much greater concentration of field at their crests than longer wavelengths, and thus have a greater difference in field between the peak and foot of a wave, more rapid smoothing is to be expected. This has been shown above.

For long-wavelength irregularities, $d\epsilon/dt$ may be found as a first approximation from Ohm's law, assuming a parallel field distribution. At the top of the wave, the field is $V/(p - \epsilon)$, and at the foot it is $V/(p + \epsilon)$. The rate of reduction of the furrow size is

$$\begin{aligned} \frac{d(2\epsilon)}{dt} &= -M \left(\frac{V}{p - \epsilon} - \frac{V}{p + \epsilon} \right) \\ \frac{d\epsilon}{dt} &= -\frac{MV\epsilon}{p^2} \end{aligned} \quad (6.35)$$

Comparing Equation (6.35) with (6.28) for the sinusoidal surface, we see that, when the wavelength is large compared to the gap ($kp \ll 1$, and $\coth kp \approx 1/kp$), Equation (6.28) reduces to (6.35), i.e. the differential equations derived in the present theory reduce to the simple ohmic equations when the conditions justify the use of the approximations of parallel field theory.

Consider Equation (6.28) when the wavelength is moderately large compared with p . Then

$$\coth kp \approx \frac{1}{kp} + \frac{kp}{3}$$

Equation (6.28) becomes

$$\frac{d\epsilon}{dt} = -MV \left(\frac{1}{p^2} + \frac{k^2}{3} \right) \epsilon$$

When the gap remains constant, integration gives

$$\epsilon = \epsilon(0) \exp\left(-\frac{MV}{p^2} - \frac{MVk^2}{3}\right)t$$

The term $\exp[-(MVk^2/3)t]$ may be regarded as a first field-concentration correction. In this case the wavelength, while still large, is sufficiently small to cause an appreciable field-concentration effect. Note that this term is independent of p , i.e. the increase in the smoothing rate, due to field concentration, surprisingly is independent of the gap width.

6.7 Surface smoothing to a required tolerance

This work has provided further information about a feature of electrochemical deburring [4]. With this process, it is useful to know the overall depth of metal which has to be machined to permit the removal of a surface irregularity, the so-called 'memory

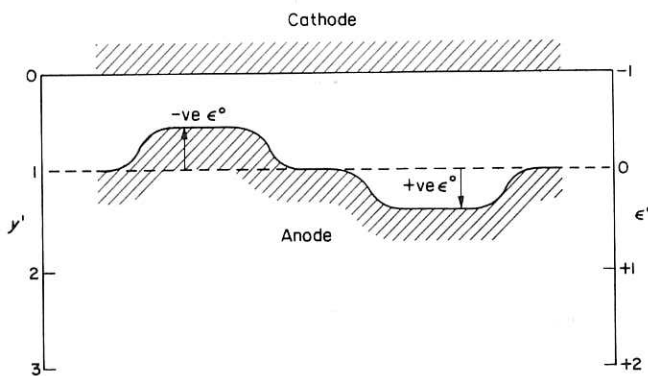


Fig. 6.3 Anode irregularities (after Tipton [5])

effect'. One of the first reports of studies on this topic is that by Tipton [5].

In this investigation, a plane cathode is again used to produce a plane surface on the anode. The latter electrode is assumed to carry initially irregularities whose surfaces are plane-faced (Fig. 6.3). That figure shows two such anodic irregularities, which are at different distances from the cathode, and assumed to be sufficiently distant from each other. Then, simple ohmic theory, incorporating parallel field lines across the gap, can be applied separately to each irregularity. As ECM proceeds, the distance from the cathode of each region of irregularity will tend to the equilibrium value. This equilibrium distance is, of course, $MV/f = h_e$. If we work in terms of dimensionless quantities, h^0 and t^0 , where

$$h^0 = \frac{fh}{MV} = \frac{h}{h_e} \quad (6.36)$$

and t^0 is the time taken to move one equilibrium gap distance:

$$t^0 = \frac{f^2 t}{MV} \quad (6.37)$$

The usual equation for the gap now becomes

$$t^0 = h^0(0) - h^0 + \ln \frac{h^0(0) - 1}{h^0 - 1} \quad (6.38)$$

The steady-state position, $h^0 = 1$, can now be considered to be the final anode surface determined by the cathode surface. The deviations from this ideal surface by the irregularities can now be expressed non-dimensionally

$$\epsilon^0 = h^0 - 1$$

Clearly, the above equation (6.38) for h^0 can be expressed in terms of ϵ^0 :

$$t^0 = \epsilon^0(0) - \epsilon^0 + \ln \frac{\epsilon^0(0)}{\epsilon^0 - 1} \quad (6.39)$$

Next, the time required to machine the anode to a required accuracy, or tolerance, can be found. For instance, suppose that the equilibrium gap is 0.5 mm and that the required tolerance is 0.05 mm. In units of the equilibrium gap, this tolerance is 0.1. The time needed to machine sufficient depth of metal to reduce an irregularity of initial size $\epsilon^0(0)$ to a required size ϵ^0 can be calculated directly from Equation (6.39). Figure 6.4 shows results for small initial irregularities (in terms of equilibrium gaps). The required depth of machining is seen to be very dependent on the required tolerance. For large initial irregularities, the height of the irregularity must be machined; in addition, a further small depth of metal, equal to $\ln[\epsilon^0(0)/\epsilon^0] - \epsilon^0$,

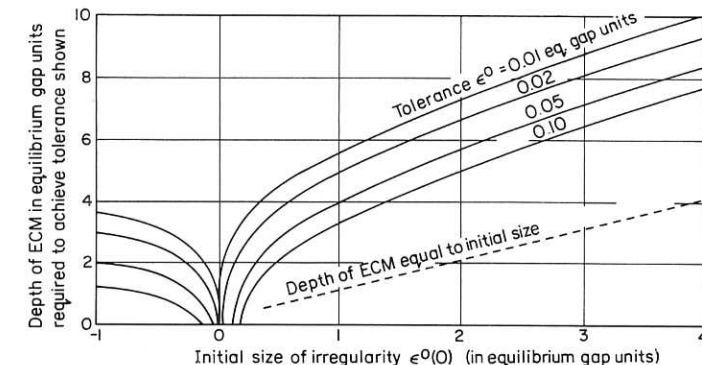


Fig. 6.4 Depth of ECM necessary to reduce small initial defects of size $\epsilon^0(0)$ to required tolerance (after Tipton [5])

must be machined. In Fig. 6.5 this additional depth of metal which must be machined for large heights of irregularities is also presented.

The difficulty of the anodic smoothing of small irregularities to a required tolerance becomes apparent from this analysis. But the

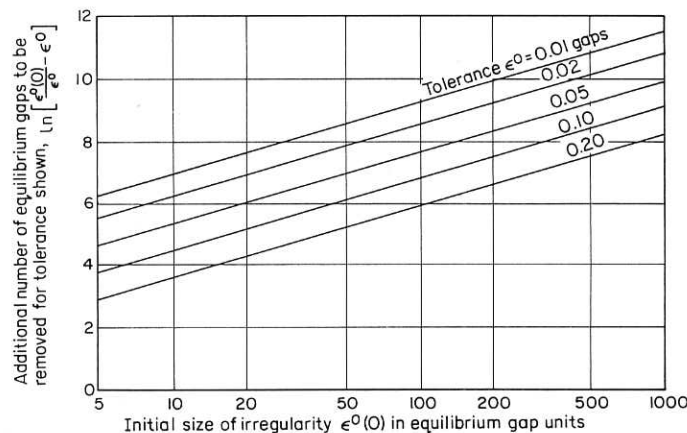


Fig. 6.5 Additional depth of ECM, $\ln[\epsilon^0(0)/\epsilon^0 - \epsilon^0]$, in excess of the original defect size necessary to reduce a large initial defect $\epsilon^0(0)$ to a specified tolerance of ϵ^0 (after Tipton [5])

preceding studies indicate a possible means of smoothing to a required tolerance under non-equilibrium ECM conditions so that a minimum amount of metal is lost.

Consider, first, short-wavelength irregularities: $kp \gg 1$ and $\coth kp \approx 1$. If the position of the average anode surface is denoted by the coordinate s , relative to a *fixed* origin, then

$$\frac{ds}{dt} = \frac{MV}{p} \quad (6.40)$$

But

$$\frac{d\epsilon}{dt} = -\frac{MVK}{p}\epsilon$$

so that

$$\frac{ds}{d\epsilon} = -\frac{1}{k\epsilon}$$

That is,

$$s = s(0) + \ln\left[\frac{\epsilon(0)}{\epsilon}\right]^{1/k} \quad (6.41)$$

where $s(0)$ is the initial value of s . Thus s has no explicit dependence on the behaviour of p , and these equations hold for both equilibrium and non-equilibrium conditions. In this case, therefore, surface irregularities cannot be reduced at a rate greater than that achieved in equilibrium conditions. That is, there is no possibility of reducing the loss of the bulk anode metal.

Next, consider the long-wavelength case: $kp \ll 1$ and $\coth kp \approx 1/kp$. Since

$$\frac{d\epsilon}{dt} = -\frac{MV}{p^2}\epsilon$$

But by means of Equation (6.40),

$$\frac{ds}{d\epsilon} = -\frac{p}{\epsilon}$$

That is,

$$|ds| = p \frac{|d\epsilon|}{\epsilon}$$

For a reduction $d\epsilon$ in the size of the surface irregularities, a corresponding lowering ds of the anode surface has to occur. The smaller the value of the mean gap width, p , the smaller will be this amount ds of bulk anode recession.

6.8 Three-dimensional anode irregularities

These can be treated by a method similar to that given above; the anode surface is described by

$$y_a = p + \epsilon \sin kx \sin lz$$

where l is the wave number of the irregularities in the z direction (perpendicular to the x, y plane). The potential is also deduced by the same procedure:

$$\phi = \frac{Vy}{p} - \frac{V\epsilon}{p} \frac{\sin kx \sin lz \sinh[\sqrt{(k^2 + l^2)}y]}{\sinh[\sqrt{(k^2 + l^2)}p]} \quad (6.42)$$

as are the equations for p and ϵ :

$$\frac{dp}{dt} = \frac{MV}{p} - f \quad (6.43)$$

$$\frac{d\epsilon}{dt} = -\frac{MV\sqrt{(l^2 + k^2)}}{p} \coth[\sqrt{(l^2 + k^2)}p]\epsilon \quad (6.44)$$

The behaviour of the anode surface is entirely similar to that of the two-dimensional surface described above. Smoothing here will be more rapid; this is to be expected, since the field concentration at the 'hills' will be greater than that around 'troughs'.

6.9 Arbitrarily shaped irregularities

The theory presented above can be extended, by the use of Fourier series, to cover any shape of anode irregularity. Detailed analysis of this treatment is available elsewhere [3]. For brevity here, only the significant results are quoted. Suppose the irregularities are described by Fourier sine series (although they can be described just as easily by cosine series, or by a combination of sine and cosine series). Then the Fourier coefficients can be shown to behave independently, and the electric field can be obtained by linear superposition of components derived from the individual Fourier terms.

Although the plane cathode is still given by $y = 0$, the anode is now described in terms of a Fourier series:

$$y = p + \epsilon(0) \sum_1^{\infty} a_n \sin \frac{n\pi x}{\lambda} \quad (6.45)$$

where 2λ is the fundamental wavelength of the irregularities, and the wave number k has been replaced by $n\pi/\lambda$; a_n is the Fourier coefficient. As usual, we assume that

$$\epsilon = \left[\epsilon(0)^2 \sum_1^{\infty} |a_n|^2 \right]^{1/2} \ll p$$

where ϵ represents the maximum amplitude of the irregularities. Here $\epsilon(0)$ is a scaling factor for the initial anode shape.

The coefficients a_n are considered to be time-dependent, and differential equations are derived for them. These equations enable description of the time-dependence of the overall height of the

irregularities and also of the variation of the shape of the anode surface with machining time.

Analysis, similar to that in Section 6.4, yields the usual expression for the rate of change of gap:

$$\frac{dp}{dt} = \frac{MV}{p} - f$$

and a differential equation for the coefficients a_n :

$$\frac{da_n}{dt} = -\frac{MV\pi}{p\lambda} n a_n \coth \frac{n\pi p}{\lambda} \quad (6.46)$$

Again, as in Section 6.5, and p being assumed constant, two limiting cases can be considered.

(i) Wavelengths small compared with the gap, i.e.

$$\frac{n\pi p}{\lambda} \gg 1, \quad \text{so that } \coth \frac{n\pi p}{\lambda} \approx 1.$$

Integration of the above equation yields

$$a_n(t) = a_n(0) \exp \left(-\frac{MVn\pi}{p\lambda} t \right) \quad (6.47)$$

From this result, we deduce that the shape of an arbitrary irregularity becomes that of a sinusoidal one with the fundamental wavelength.

(ii) Wavelengths large compared with the gap, i.e.

$$\frac{n\pi p}{\lambda} \ll 1, \quad \text{so that } \coth \frac{n\pi p}{\lambda} \approx \frac{\lambda}{n\pi p}$$

On integration of Equation (6.46),

$$a_n(t) = a_n(0) \exp \left(-\frac{MV}{p^2} t \right) \quad (6.48)$$

This result is the simple ohmic one, previously derived.

6.10 Extension of above theory for even and arbitrarily shaped irregularities

Results similar to those of Section 6.5 can be obtained for irregularities represented by a Fourier cosine series (e.g. cusp-shaped irregularities).

Suppose that the anode is represented by

$$y_a = h(t) - a_0 \epsilon(0) - \epsilon(0) \sum_1^{\infty} a_n(t) \cos \frac{n\pi x}{\lambda} \quad (6.49)$$

Clearly, $p(t)$ is now represented by $h(t) - \epsilon(0)a_0(t)$, and the anode surface is not symmetric about the line defined by the average gap p , as was the case previously. However, similar equations for $a_n(t)$ can be deduced, and for the symmetric case, the expression for $\epsilon(t)$ is

$$\epsilon(t) = \epsilon(0) \sum_1^{\infty} a_{2n-1}(t) \quad (6.50)$$

When the top and foot of the irregularities do not occur at the positions of symmetry, the anode shape may be represented by a general Fourier series:

$$y_a = p(t) + \epsilon(0) \sum_1^{\infty} a_n \cos \frac{n\pi x}{\lambda} + \epsilon(0) \sum_1^{\infty} b_n \sin \frac{n\pi x}{\lambda} \quad (6.51)$$

If the top and foot occur at $x = \alpha$ and $x = \beta$ respectively, the height of the irregularities is

$$\epsilon(t) = \epsilon(0) \sum_1^{\infty} a_n \left(\cos \frac{n\pi \beta}{\lambda} - \cos \frac{n\pi \alpha}{\lambda} \right) + \epsilon(0) \sum_1^{\infty} b_n \left(\sin \frac{n\pi \beta}{\lambda} - \sin \frac{n\pi \alpha}{\lambda} \right) \quad (6.52)$$

In general, α and β will be functions of time; this is to be expected, since the shape of the irregularity will change to a sinusoidal one, with the basic wavelength.

Example

Suppose the irregularities consist of a series of rectangular steps, $\epsilon(0)$ being the initial step height. Then

$$a_n(0) = \begin{cases} \frac{2}{n\pi}, & n \text{ odd} \\ 0, & n \text{ even} \end{cases}$$

If the basic wavelength 2λ is assumed sufficiently large so that the long-wavelength approximation may be used for each component, then

$$a_n(t) = \frac{2}{\pi n} \exp \left(-\frac{MV}{p} t \right)$$

for n odd. We obtain that (for constant p)

$$\begin{aligned} \epsilon(t) &= \frac{4\epsilon(0)}{\pi} \exp \left(-\frac{MV}{p^2} t \right) \sum_1^{\infty} (-1)^r \frac{1}{2r+1} \\ &= \epsilon(0) \exp \left(-\frac{MV}{p^2} t \right) \end{aligned}$$

since

$$\sum_1^{\infty} (-1)^r \frac{1}{2r+1} = \frac{\pi}{4}$$

This is the ohmic result and is to be expected, since a long-wavelength step is a case where the basic ohmic theory will be reasonably accurate.

Figure 6.6 shows how the rectangular step changes with time to a sinusoidal irregularity. Notice here that the theory predicts an initial virtual growth of the anode at the base of the step; this is due to a breakdown of the linearization approximation near areas of abrupt change of anode slope. However, it is shown later that such areas are rapidly removed; thus the above theoretical paradox has negligible bearing on the subsequent changes of the anode profile.

Shapes for which the coefficients of the higher harmonic terms are appreciable in comparison with those of the basic terms will be smoothed rapidly, for the higher harmonic (shorter wavelength) terms are reduced most rapidly. If the effect of shape and spacing of irregularities on smoothing time is investigated, sharp profiles

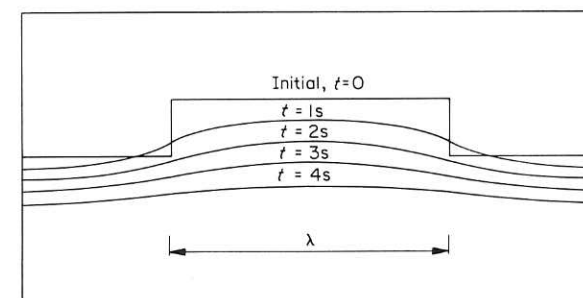


Fig. 6.6 Successive anode profiles during smoothing of initially rectangular step (after Fitz-Gerald and McGeough [3])

will be shown to dissolve more quickly than those which are less sharp, and widely spaced irregularities will be dissolved more rapidly than those close together (the basic shape being the same in all cases). Numerical illustrations of such considerations are now given.

Examples

Typical values used for the various constants are: $V = 10$ V, $p = 0.5$ mm, $f = 5.67 \times 10^{-3}$ mm/s, $M = 1.7 \times 10^{-5}$ cm² V⁻¹ s⁻¹.

(i) Consider first the smoothing of cusp-shaped irregularities described by

$$y_a = h - \frac{\epsilon(0)x^4}{\lambda^4} \quad (-\lambda \leq x \leq \lambda)$$

with the same notation as before. We use a cosine expansion:

$$y_a = p(t) + \epsilon(0) \sum_1^{\infty} a_n(t) \cos \frac{n\pi x}{\lambda}$$

where

$$a_n(0) = \frac{8(-1)^n}{(n\pi)^4} [(n\pi)^2 - 6] \quad (n \neq 0)$$

For $2\lambda = 10^{-1}$ mm, the time dependence of ϵ is shown in Fig. 6.7. For comparison, the behaviour of a sinusoidal irregularity of the

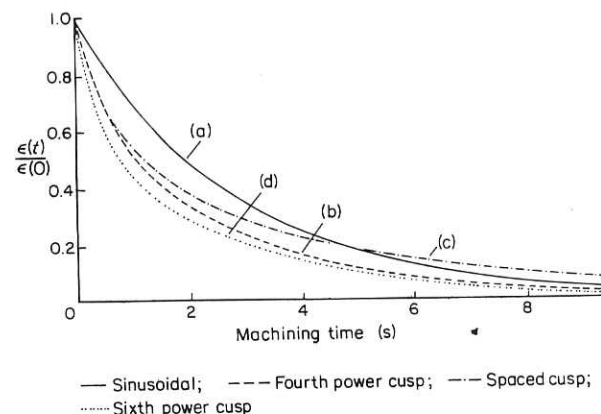


Fig. 6.7 Decrease in height of irregularities with time, showing dependence of smoothing times on shape and spacing: (a) sinusoidal; (b) fourth power cusp; (c) spaced cusp; (d) sixth power cusp (after Fitz-Gerald and McGeough [3])

same wavelength is also given. Table 6.1 shows the initial odd coefficients (which determine the height of the irregularities).

Table 6.1 Initial odd Fourier coefficients for cusp-shaped irregularity. [Section 6.10.
Example (i)]

$a_1 = 0.316$	$a_9 = 0.010$
$a_3 = 0.084$	$a_{11} = 0.007$
$a_5 = 0.031$	$a_{13} = 0.005$
$a_7 = 0.016$	$a_{15} = 0.004$

(ii) Separation of the cusps by plane segments of length 2λ is next considered. The basic wavelength is now 0.2 mm. The relevant Fourier coefficients are given in Table 6.2.

Table 6.2 Initial Fourier coefficients. [Section 6.10.
Example (ii)]

$a_1 = 0.188$	$a_9 = 0.019$
$a_3 = 0.121$	$a_{11} = 0.013$
$a_5 = 0.058$	$a_{13} = 0.009$
$a_7 = 0.031$	$a_{15} = 0.007$

Note that the higher harmonics are relatively more important in this case. Initially, smoothing will be faster since there is a greater field concentration. Later, as the shape approaches the basic sinusoidal form, the rate of smoothing will decrease; since the basic wavelength is double that of the unseparated cusps, the rate will be less than the rate for the unseparated cusps (Fig. 6.7). It will be noted that, for this wavelength, the initially greater smoothing rate persists for only half a second. This effect is more pronounced for longer wavelengths, and Fig. 6.8 shows the comparison for a basic wavelength of 40 mm (an extreme case).

(iii) The effect of shape, as distinct from spacing, on the smoothing rate for the cusps is now considered. The results obtained from example (i) will be compared with those for a sharper cusp, whose initial shape is described by:

$$y_a = p(0) - \epsilon(0) \frac{x^6}{\lambda^6} \quad (-\lambda \leq x \leq \lambda)$$

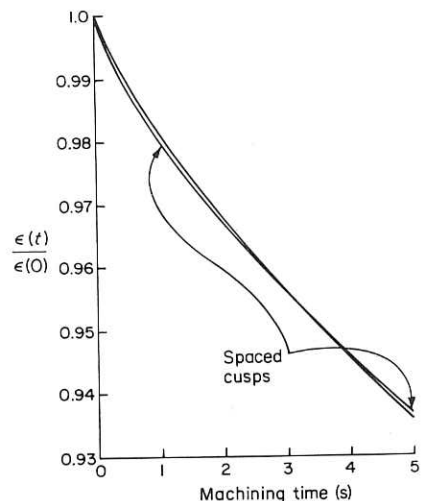


Fig. 6.8 Dependence of spacing for fourth power cusps of relatively long wavelength ($2\lambda = 40$ mm) (after Fitz-Gerald and McGeough [3])

again with $2\lambda = 10^{-1}$ mm. The Fourier coefficients are given in Table 6.3. The higher harmonics are again of greater importance; smoothing will again be faster than in (i) (Fig. 6.7).

Table 6.3 Initial Fourier coefficients. [Section 6.10. Example (iii)]

$a_1 = 0.250$	$a_9 = 0.015$
$a_3 = 0.107$	$a_{11} = 0.010$
$a_5 = 0.045$	$a_{13} = 0.007$
$a_7 = 0.024$	$a_{15} = 0.005$

(iv) Finally, the smoothing of a sinusoidal and a square-wave rectangular irregularity of the same wavelength is considered (Fig. 6.9). Since there is less field concentration at the middle of the square wave, its smoothing rate will be smaller. The behaviour of a

Table 6.4 Fourier coefficients. [Section 6.10. Example (iv)]

$a_1 = 0.637$	$a_9 = 0.071$	$a_1 = 0.551$	$a_9 = 0.000$
$a_3 = -0.212$	$a_{11} = -0.058$	$a_3 = 0.000$	$a_{11} = -0.050$
$a_5 = 0.127$	$a_{13} = 0.049$	$a_5 = -0.110$	$a_{13} = 0.042$
$a_7 = -0.091$	$a_{15} = -0.042$	$a_7 = 0.079$	$a_{15} = 0.000$
Equally spaced		Separated	

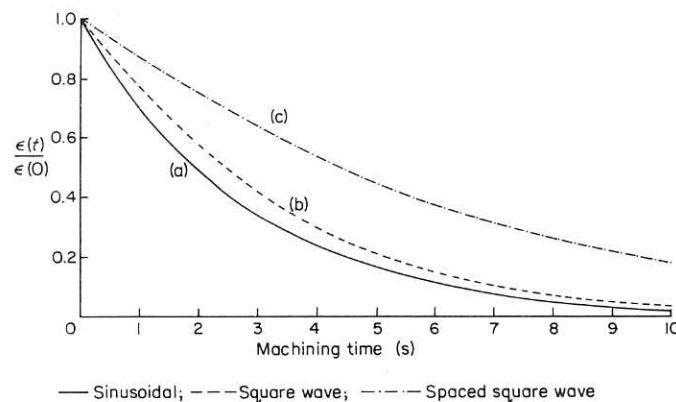


Fig. 6.9 Smoothing of rectangular steps, showing dependence on spacing; the curve for a sinusoidal wave is shown for comparison; (a) sinusoidal, (b) square wave, (c) spaced square wave (after Fitz-Gerald and McGeough [3])

spaced square wave is also given; in this case, no indication of the initially greater smoothing rate found for the cusp example is seen, and even for a wavelength of 1 mm the smoothing rate is always smaller. Table 6.4 shows a comparison between the Fourier coefficients for equally spaced, and separated, square waves.

6.11 The effects of overpotentials

6.11.1 Overpotentials only at the cathode

For clarity, the effect of an overpotential only at the cathode is initially considered. From Section 6.2, the boundary condition for the potential at the cathode is now given as $\phi = f(J)$. Expanding $f(J)$ as a Taylor series, we obtain

$$\begin{aligned}\phi &= f(J) + \left. \frac{\partial f}{\partial J} \right|_{J=\bar{J}} (J - \bar{J}) \\ &= \alpha + \beta(J - \bar{J})\end{aligned}\quad (6.53)$$

where \bar{J} is the average current density, α (the average overpotential) is $f(\bar{J})$, and

$$\beta = \left. \frac{\partial f}{\partial J} \right|_{J=\bar{J}} \quad (6.54)$$

The small difference between the current density, J , and the average current density is a consequence of the overpotential.

Because of the overpotential, the previous expression for the potential, Equation (6.22), must be modified. It is possible to consider the effect to be 'reflected' from the anode; the shape variations on the anode cause variations in the field concentrations there, and these in turn create small variations in the current density at the cathode. It is therefore plausible to consider a new potential of the form

$$\phi = A + \frac{V - A}{p} \times \left\{ y - \epsilon(0) \sum_{n=1}^{\infty} \sin \frac{n\pi x}{\lambda} \frac{a_n \sinh(n\pi y/\lambda) + b_n \sinh[n\pi(p-y)/\lambda]}{\sinh(n\pi p/\lambda)} \right\} \quad (6.55)$$

where A and b_n are to be determined.

An analysis of the problem has been set out by Fitz-Gerald and McGeough [3]. Again, for brevity, only the salient results are given here.

Owing to overpotential, the usual equation for the variation in gap width becomes modified:

$$\frac{dp}{dt} = M \left(\frac{V - A}{p} \right) - f \quad (6.56)$$

in which it can be shown that $A = \alpha$, the average overpotential.

From Equation (6.56), the condition for the equilibrium gap is now

$$f = \frac{MV}{p} - \frac{MA}{p} \quad (6.57)$$

Clearly, the feed-rate required for a specified gap is now reduced by an amount MA/p . A slower anode dissolution rate then occurs, and consequently a slower overall reduction rate of the height of the irregularities.

Example

Suppose $f(J) = bJ$ (low current density form of Tafel's relationship). Then, in Equation (6.53) $\alpha = b\bar{J}$ and $\beta = b$; and now Equations (6.53) and (6.56) yield

$$\frac{dp}{dt} = \frac{MV}{p + b\kappa_e} - f$$

i.e. the effect is to increase the effective gap width by a factor $(1 + b\kappa_e/p)$. Alternatively, the time required to achieve the equilibrium gap will be increased. The significance in electrodeposition of the quantity b has been fully recognised by, for example, Kasper [6-8] and Hoar and Agar [9].

The presence of overpotentials also causes an alteration in the Fourier coefficients which are used to describe the anode surface. For constant p and for odd-shaped irregularities, these coefficients are altered to

$$a_n(t) = a_n(0) \exp \left[-\frac{M(V - A)}{p} \frac{n\pi}{\lambda} \coth \frac{n\pi p}{\lambda} \omega(p)t \right] \quad (6.58)$$

where $\omega(p)$ is a correction factor for the overpotential.

Fitz-Gerald and McGeough discuss two particular conditions for $\omega(p)$. When the irregularities are of long wavelength,

$$\omega = \left(1 + \frac{\mu}{\sigma} \right)^{-1} \quad (6.59)$$

For convenience, two dimensionless parameters have been introduced:

$$\sigma = p/\lambda \quad \text{the configuration parameter}$$

$$\mu = \beta\kappa_e/\lambda \quad \text{the overpotential parameter}$$

For $\mu/\sigma \ll 1$, $\omega \approx (1 - \mu/\sigma)$, which introduces a small correction to the smoothing time. For $\mu/\sigma \gg 1$, however, as here, long-wavelength irregularities (or components) are dissolved very slowly; smoothing is then difficult. (Note: a corresponding situation in electrodeposition has been discussed fully by Wagner [10].)

In the short-wavelength case, ω becomes

$$\omega = \frac{1 + n\pi\mu(1 - 4e^{-2n\pi\sigma})}{1 + n\pi\mu} \quad (6.60)$$

If $n\pi\mu \ll 1$, this gives $\omega = 1 - 4n\pi\mu e^{-2n\pi\sigma}$, while for $n\pi\mu \gg 1$, $\omega = 1 - 4e^{-2n\pi\sigma}$. In both cases, ω is negligibly different from unity, in view of the short-wavelength assumption. These short-wavelength irregularities are therefore unaffected by the fluctuations in the overpotential, although the time constant for their rate of removal is increased by a factor $V/(V - A)$.

The overall effect of a current density-dependent overpotential, then, is to produce waves of relatively long wavelength on the smoothed surface. The persistence of these waves depends on the

value of μ/σ , as demonstrated in the long-wavelength case above. The effect may be diminished by either (a) reducing κ_e or (b) increasing p (or decreasing the feed-rate f). Both of these remedies have the unwanted side-effect of reducing the current, so that elimination of overpotential effects may only be obtained at the expense of increased smoothing time.

6.11.2 Overpotentials at both electrodes

If now overpotentials on both anode and cathode are to be considered, the boundary conditions become

$$\phi = f(J) \quad \text{on the cathode}$$

$$\phi = V - g(J) \quad \text{on the anode}$$

As before, $f(J)$ and $g(J)$ are expanded as Taylor series, and all but the first two terms of each are neglected.

$$f(J) = \alpha + \beta(J - \bar{J}) \quad (6.61)$$

$$g(J) = \gamma + \tau(J - \bar{J}) \quad (6.62)$$

where α and β are defined as before, and $\gamma = g(\bar{J})$, $\tau = \partial g / \partial J|_{J=\bar{J}}$.

By arguments similar to those already outlined, it can be postulated that effects of these overpotentials can be described in terms of two additional Fourier coefficients b_n and c_n , and overpotential parameters, μ and σ , defined above, and $\nu = \tau\kappa_e/\lambda$.

6.11.3 Overpotentials only at the anode

The condition $\nu \ll \mu$ corresponds to overpotentials only at the cathode. Their effects have been discussed. However, if $\nu \gg \mu$, it can be shown that in the limiting case, $\mu/\nu \rightarrow 0$,

$$b_n = 0$$

$$c_n = -a_n \frac{n\pi\nu}{\tanh n\pi\sigma + n\pi\nu} \quad (6.63)$$

The case now is that of overpotential only at the anode. For long wavelengths,

$$c_n = -a_n \frac{\nu}{\sigma + \nu} \quad (6.64)$$

and the behaviour is similar to that in the corresponding case discussed above.

The short-wavelength case, however, gives

$$c_n = -a_n \frac{n\pi\nu}{1 + n\pi\nu} \quad (6.65)$$

Whereas previously the overpotential had little or no effect on the short-wavelength irregularities (other than the overall rate reduction), the large overpotential case ($\nu \gg 1$) gives

$$c_n \approx -a_n$$

yielding

$$\frac{da_n}{dt} \approx 0 \quad (6.66)$$

for all n . Thus the reduction rate for all Fourier components is very small; the anode profile is 'frozen' as the surface is machined away. Even in the case $\nu \ll 1$, when the effect on the long wavelengths decreases, for suitably large n , $da_n/dt \rightarrow 0$; in this situation, the short-wavelength components are preferred to the long-wavelength ones.

An experimental verification of this theory remains to be published. The results, however, do demonstrate the type of analysis required for the shaping problem in ECM. In addition, the investigation of overpotentials indicates the effects which might be encountered in ECM, particularly since close resemblance is obtained between these results and those already found theoretically and experimentally in electrodeposition.

References

1. McGeough, J. A. and Rasmussen, H., *J. Inst. Maths. and Applics.* (1974) 1, 13.
2. Rasmussen, H. (in preparation).
3. Fitz-Gerald, J. M. and McGeough, J. A., *J. Inst. Maths and Applics.* (1969) 5, 389.
4. Warburton, P. and Sadler, B., Paper presented at First Int. Conf. on ECM, Leicester University, Mar. 1973.
5. Tipton, H., Proc. Fifth Int. Conf. Mach. Tool Res., Birmingham (1964) Sept., p. 509.
6. Kasper, C., *Trans. Electrochem. Soc.* (1940) 77, 353, 365.
7. Kasper, C., *Trans. Electrochem. Soc.* (1940) 78, 131, 147.
8. Kasper, C., *Trans. Electrochem. Soc.* (1942) 82, 153.
9. Hoar, T. P. and Agar, J. N., *Discuss. Faraday Soc.* (1947) 1, 162.
10. Wagner, C., *J. Electrochem. Soc.* (1951) 98, 116.